International Journal of Nanoelectronics and Materials
IJNeaM
ISSN 198-5761 | E-ISSN 2232-1535

Nitrogen-doped Graphene/Natural Rubber and Sodium Dodecyl Sulfate Modified Nanocomposites: Study on the Electrochemical Properties for the Potential Sensor Response

Md. Shalauddin[a], Ab Rahman Marlinda[a,*], Azim Danial Azam[a], Vishnukumar Rajandran[a] and A. A Saifizul[b,*]

[a]*Nanotechnology and Catalysis Research Centre (NANOCAT), Universiti Malaya, 50603 Kuala Lumpur, Malaysia.*
[b]*Mechanical Engineering Department, Faculty of Engineering, Universiti Malaya, 50603 Kuala Lumpur, Malaysia.*
**Corresponding authors e-mail:* marlinda@um.edu.my* saifizul@um.edu.my*

ABSTRACT

In this study, a piezoelectric composite was developed based on nitrogen-doped graphene/natural rubber (NGr-NR) and an anionic surfactant sodium dodecyl sulfate (SDS) through a simple sonication method. Taking advantage of the high electrical conductivity and high surface area of NGr, the hybrid network of NGr-NR-SDS nanocomposite showed excellent mechanical properties and enhanced electrochemical behavior. Here, NGr was used as functional filler materials incorporated into NR polymeric matrix. SDS was used with NGr-NR composite to reduce the aggregation and promote the interfacial interaction between NGr-NR which enhanced the stability of sensor. The surface morphology of NGr-NR-SDS was investigated by field emission scanning electron microscopy, transmission emission microscopy, and Fourier transform infrared spectroscopy. Cyclic voltammetry and electrochemical impedance spectroscopy of NGr-NR-SDS showed the highest current response of 17 μA and the lowest R_{ct} value of 1920 Ω demonstrating the excellent electrochemical response. The significance of this result is that the developed nanocomposite shows great potential for flexible piezoelectric devices due to excellent electrochemical response and cyclic stability.

Keywords: *Nitrogen-doped Graphene, Natural Rubber, Sodium Dodecyl Sulfate, electrochemical analysis, piezoelectric response*

1. INTRODUCTION

Nitrogen-doped graphene (NGr) consists of a single layer of sp2 hybridized carbon atoms with the doping of nitrogen atoms on the layer of graphene (Gr) sheets which possess all the distinct characteristics of Gr with high surface area, excellent electrical conductivity [1]. In addition, NGr minimizes the restacking problems during the π-π interactions and enhances the accessibility of the analytes in the active site. Due to these fascinating properties, NGr has great potential for application in piezoelectric sensors, piezoresistive sensors, pressure sensors, and so on [2, 3].

Natural rubber (NR) obtained from plant sources is an eco-friendly and cost-efficient polymer. The production of NR is easy and facile. The sustainability with its outstanding mechanical features including stretchability and flexibility makes NR an attractive option for versatile applications including flexible strain sensors. The flexible architecture of NR facilitates the deposition of carbon nanostructured materials on the surface of NR [4]. Previously, some researchers developed several novel approaches to synthesize NR-based composite integrating carbon nanostructured filler such as carbon nanotubes, graphene related materials containing three-dimensional (3D) configuration. This process includes the dispersion of the filler into the NR polymeric matrix and assembles on the NR surface. The integration of carbon nanostructured filler and NR polymer shows several advantages such as preventing the aggregation of carbon nanomaterials and enhancing the conductivity of the composite by offering a 3D network with the encapsulation of filler material and strongly attached with the interstices of NR particles which allows a continuous rubbery phase with homogenous dispersion of carbon nanostructured filler [5, 6].

Sodium dodecyl sulfate (SDS) is known as an anionic surfactant that modifies the physicochemical properties of the modified electrode. [7]. SDS mainly possesses the ability to minimize the surface tension and enhance the dispersing ability of any heterogeneous mixture, offers a continuous distribution of the nanoparticles, and facilitates the attachment of the nanoparticles by minimizing the surface tension of the electrode-electrolyte surface [8]. In the NGr-NR-SDS composite, SDS ensures the uniform dispersion of NGr on the NR polymeric matrix.

Huang et al reported a composite of extremely elastic and conductive N-doped graphene sponge for monitoring of human motions with excellent electrical conductivity (1.4 S m^{-1}), as well as remarkable sensing performances with high sensitivity (1.33 kP^{-1}), low detection limit (2% strain), excellent linear sensing range (nearly 20%), long term stability (3000 cycles), and fast response (72.4 m s) [9]. While Liu et al developed a nanocomposite of MXene and NGR as a piezoresistive sensor with high sensitivity of 0.21 kPa^{-1} at a pressure range of 0–2 kPa for piezoresistive sensing with superior durability over 2000 cycles [10] . According to previous works, the homogeneous

preparation of composite containing carbon-based nanofiller and NR has become a challenging issue. As the carbon nanofillers are lightweight and NR is a comparatively heavy and concentrated polymer material, so proper dispersion of carbon nanostructured filler within the NR matrix is a challenging task. In addition, to ensure the stability of the prepared composite, employing surfactants is an effective approach. SDS has the capability to reduce the agglomeration of the nanomaterials and assure the homogeneous dispersion of the carbon filler and NR by eliminating the surface tension. Thus, SDS contributes for the high stability of the prepared composites [11-13]. Till now, no works have been reported on the NGr-NR-SDS composite to investigate the piezoelectric properties.

In the present study, we have constructed a novel composite of NGr-NR-SDS by utilizing solution blending and ultrasonication method. The as prepared material was investigated to study the potential of piezoelectric characteristics. The combination of the extra-ordinary electrical and high mechanical properties of NGr and high stretchability of NR contributed to the excellent piezoelectric properties, high flexibility, and outstanding cyclic stability. In addition, the NGr-NR-SDS composite showed distinct current response and low charge transfer resistance demonstrating high electroconductivity of the prepared composite. The findings of this study will contribute to the development of sensitive, reliable, and cost-effective piezoelectric composite for various and versatile applications.

2. EXPERIMENTAL

2.1 Chemicals and Instruments

2.1.1 Chemicals

Natural rubber (CV-60 dry rubber) was provided by the Malaysia Rubber Board, Malaysia. Graphene oxide (GO) (99.5%) and hydrazine hydrate (80%) were purchased from Sigma Aldrich, Malaysia. The source of toluene (99%) was Merck in Germany. Potassium ferricyanide (99%), potassium ferrocyanide [$K_4Fe(CN)_6$] (99%) and potassium chloride (KCl) (99.9%) were delivered by Tianjin Broadcom Chemical Co., Ltd. (Tianjin, China). Since the solvents and reagents are analytical grade, they don't require additional purification before use.

2.1.2 Instrumentations

An Autolab PGSTAT302N model (Eco Chemie, Netherlands) electrochemical workstation was utilized as the electrochemical detection platform with a NGr-NR-SDS composite as the working electrode, a platinum wire as the counter electrode, and Ag/AgCl (3.0 M KCl) as a reference electrode. Every electrochemical test was carried out at room temperature. Using a PURELAB flex system (Elga Water, Veolia, France) to purify the deionized (DI) water (18.2 MΩ cm), an aqueous solution was prepared for the duration of the experiment. Fourier-transformed infrared (FTIR) spectroscopy was carried out via Spectrum 2000, Perkin Elmer, U.S. The morphological image was recorded by transmission electron microscopy (TEM) (JEM 1400, JEOL, Japan). Field emission scanning electron microscope (FESEM) of NGr-NR-SDS was investigated by JEOL JSM-7600F (Japan), attached with energy dispersive X-ray (EDX) spectrometer.

2.2. Synthesis Methods for NGr-NR-SDS Composite

2.2.1. Synthesis of NGr

NGr was synthesized using a microwave-assisted method. Graphene oxide (GO) was utilized as the initial material for this synthesis. [14]. At first, 0.35 mg mL^{-1} of GO solution was ultrasonicated for 25 min to afford a yellow-brownish dispersion. Then, 0.8 mL of hydrazine was introduced into 35 mL of GO dispersion to start the reduction process. Next, the product was irradiated for 7 min in a microwave oven to obtain the NGr solution and centrifuged for 15 min at 1000 rpm. After the supernatant was removed, the residue was gathered and dried at 50°C.

2.2.2. Preparation of NGr-NR-SDS Nanocomposite

The NGr-NR nanocomposite was obtained followed by the solution bending approach via ultrasonication. To enhance the surface area, multiple pieces of CV-60 grade NR were cut. To obtain 10% total solid content (TSC) of NGr-NR nanocomposite, 10 g NR was dispersed into 100 mL toluene. The NR was dispersed gradually into toluene and stir continuously to afford a uniform NR solution. Next, NR solution is mixed with NGr solution in different ratio which is mentioned in Table 1. To dissolve NGr into the NR solution, a standard handheld electric drill is used for one hour after using a top-down stirring technique. Next, 0.5% SDS solution was added in to NGr-NR solution to ensure the dispersion of the NGr nanomaterial into the NR matrix. The dispersion is ultrasonicated for 1 h. The uniform dispersion is then poured into a mold and dried whole night at 60ºC in an oven. Finally, a smooth surface of NGr-NR-SDS composite was obtained and the thickness of NGr-NR-SDS composite was measured as 2 mm.

Table 1 The NGr-NR-SDS composite's formulation

	NR 10% TSC 0 wt.% NGr	**NR 10% TSC 2 wt.% NGr**	**NR 10% TSC 2 wt.% NGr 0.5% SDS**
NR Solution (mL)	25	25	25
Weight of NGr (mg)	0	50	50
Weight of SDS (mg)	0	0	5

3. RESULTS AND DISCUSSION

3.1 Surface Morphology for NGr-NR-SDS Composite

FESEM was conducted to study the surface morphology of prepared composites. Figure 1A represents a thin sheet or curtain-like morphology of NR. Figure 1B is the NGr, showing a wrinkled-shaped corrugated morphology with random aggregation. Figure 1C shows the NGr-NR composite. It was observed that NGr is encapsulated within the NR polymeric matrix surface. Figure 1D is the NGr-NR-SDS composite which shows that, due to the presence of SDS, NGr is dispersed homogeneously on the NR polymeric matrix and enables an extremely porous surface. Due to the charging effect from NR, the surface of NGr-NR-SDS shows a white color appearance. SDS promotes the dispersion of the NGr-NR matrix which accelerates the electron transfer process between the surface and electrolyte. Figure 1E show the EDX analysis for the distribution of the elemental percentage of the NGr-NR-SDS composite. The inset table of Figure F shows the elemental percentage of carbon (C) is 66.4%, oxygen (O) 26.2%, nitrogen (N) 5.3%, sodium (0.8%), and sulfur (S) 0.3%. These results confirm the successful preparation of the NGr-NR-SDS composite with no impurities.

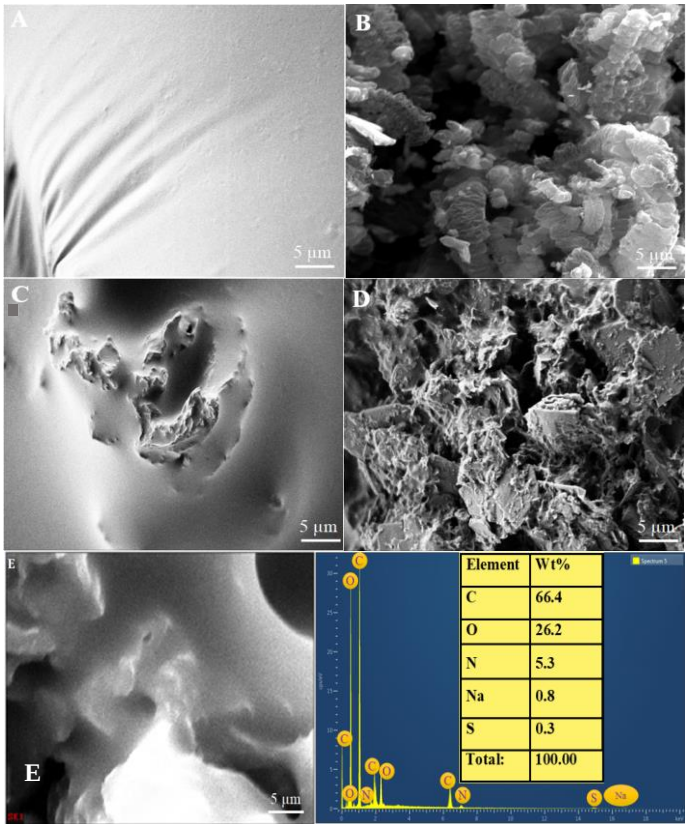

Figure 1. FESEM images for (A) NR, (B) NGr, (C) NGr-NR composite, and (D) NGr-NR-SDS composite and (E) EDX analysis for the elemental percentage in NGr-NR-SDS composite.

Figure 2A shows the TEM images of NGr-NR composite showing several agglomerations on the surface and marked with yellow color inside figure A. Figure 2B is the NGr-NR-SDS composite, a uniform dispersion of NGr-NR due to the presence of SDS demonstrating that, SDS reduces the aggregation of surface agglomeration and enhance the dispersion ability of NGr and NR and facilitates the strong interaction between NGr and NR by providing a homogeneous texture.

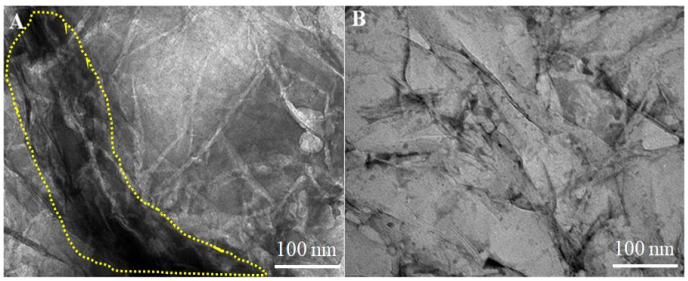

Figure 2. TEM images for (A) NGr-NR, (B) NGr-NR-SDS composite.

3.2 Functional Group Determination of NGr-NR-SDS

3.2.1 FTIR Spectroscopy

The functional group of selected nanocomposite was identified using FTIR spectroscopy. Figure 3A represents the FTIR spectra of NR. A prominent absorbance peak appeared at 3008 cm^{-1} and 2995 cm^{-1} which correspond to CH_4, and C-H groups present in CH_4. Another peak appeared at 865 cm^{-1}correspond to –C=C- functional group from C_2H_4. Because of the oxygen in NR, a sharp peak at 1670 cm^{-1} was seen, which corresponds to C=O stretching vibrations [15]. Furthermore, a peak in absorbance was seen at 1496 cm^{-1}, which is associated with the –C=C= groups found in hydrocarbons. Moreover, the absorption peak was appeared at 1448 cm^{-1} ascribed to CH_2, and at 1372 cm^{-1} ascribed to CH_3 from C_3H_6 and at 1025 cm^{-1} for –C=H- from C_4H_8 respectively [16]. The FTIR spectra of NGr are displayed in Figure 3B, where absorption peaks are centered at approximately 1138 cm^{-1} and 1512 cm^{-1}, respectively, and are attributable to the stretching vibrations of C-N and C=N. A prominent peak is centered at around 1768 cm^{-1} assigned to C=O stretch [17, 18]. However, Figure 3C curve a represents the FTIR spectrum of NGr-NR, where all the characteristic peaks were present for NGr and NR. But the absorption peak heights were reduced comparatively Figure A and B curve. This could be attributed to the attachment of NGr and NR. Furthermore, curve b is the FTIR spectrum of NGr-NR-SDS, where all the characteristic peak were observed for NGr and NR along with the characteristic peaks of SDS such as the absorption peak around approximately at 1225 cm^{-1} ascribed to the S=O stretch and absorption peak at 1071 cm^{-1} attributed to the C-C stretching [19]. Furthermore, an additional absorption peak was seen at 3445 cm^{-1}, attributed to the stretching of H-OH, as a result of the presence of SDS [20]. It is evident from the FTIR data that NGr, NR, and SDS are present in the NGr-NR-SDS composite.

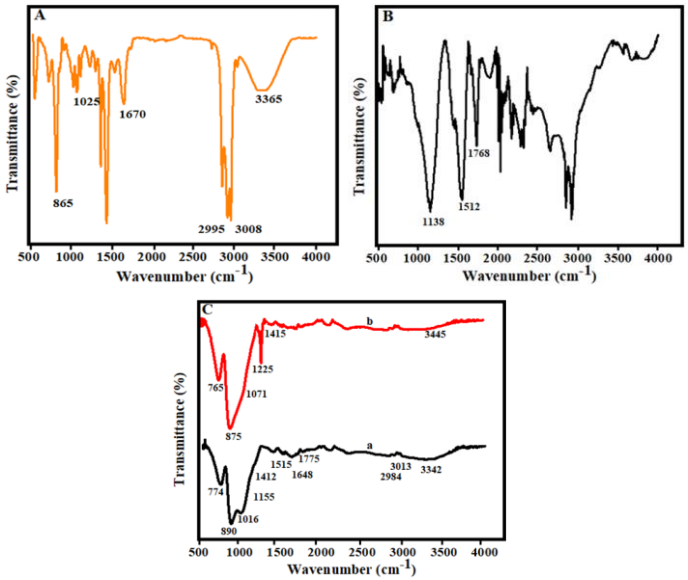

Figure 3. FTIR spectra for (A) NR, (B) NGr, and (C) NGr-NR (a) and NGr-NR-SDS (b).

3.3. Electrochemical Performance of NGr-NR-SDS

3.3.1. Electrochemical Impedance Spectroscopy (EIS) of NGr-NR-SDS

The EIS is a useful method to investigate the charge transfer kinetics of the electrode surface [21, 22]. The Nyquist curve for different prepared composites in the presence of 0.1 M KCl and 5.0 mM Fe $[CN)6]^{3-/4-}$ is displayed in Figure 4 between 100 kHz to 100 mHz. The semi-circle segment of the Nyquist curve defines the R_{ct}, while the linear segment defines the Warburg impedance which appears for diffusion of electrolyte. Based on the Nyquist plot, the charge transfer resistance (R_{ct}) values for (a) NR, (b) NGr-NR, and (c) NGr-NR-SDS are 6450 Ω, 3275 Ω, and 1920 Ω, respectively. The different values of R_{ct} for different composite can be described through different composite concentrations. Curve a shows that, the Nyquist plot of NR shows the highest R_{ct} value. As NR is an insulator, not an ion conductor. Tightly bonded electrons, which are not available for sharing by nearby atoms, are present in NR. The high resistivity of NR is influenced by the characteristics of NR, which also leads the electrons to slow down and eventually stop moving altogether.

Curve b shows comparatively lower resistivity than curve a. This could be ascribed to the integration of NGr and NR. NGr has a large surface area and strong electrical conductivity. Because of its excellent electrical conductivity and electron transport, NGr integrates well with NR, the overall conductivity of NGr-NR composite increases. That is why comparatively low R_{ct} value was obtained. Curve c shows the lowest R_{ct} value of 1920 Ω compared to curve a and b. The lowest R_{ct} value was obtained for NGr-NR-SDS composite. Due to the presence of SDS on NGr-NR composite, it reduces the surface tension which facilitates the dispersion profile of the NGr-NR composite resulting in the enhanced transfer of electrons, remarkable electrical conductivity, and lowest R_{ct} value. The Randles equivalent circuit derived from the Nyquist curves a and b is displayed in the inset image of Figure 4. Here, C_{dl} stands for double-layer capacitance, R_s for solution resistance, and R_{ct} for charge transfer resistance. It is noteworthy that, for the NGr-NR-SDS composite, the Randles equivalent circuit shows a semicircular curve with a Warburg impedance which was not observed in curves a and b. The Randles equivalent circuit obtained from the Nyquist plot for curve c, W = the Warburg impedance (Z_w) appeared along with other circuit components. The presence of Z_w demonstrates the ion diffusion on the composite surface. Therefore, it can be concluded that NGr-NR-SDS has the lowest R_{ct} value and highest electrical conductivity.

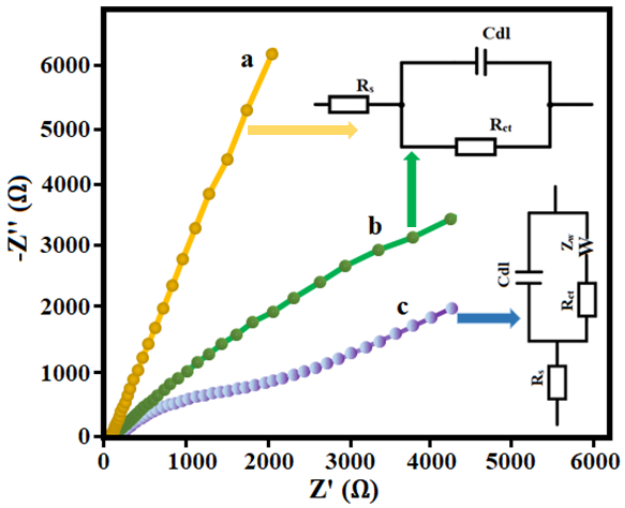

Figure 4. Nyquist plots of bare NR (a), NGr-NR (b), and NGr-NR-SDS (c) in 0.1 M KCl solution in the presence of 5.0 mM $[Fe (CN)_6]^{3-/4-}$. The analogous circuit of the fitted data is displayed in the inset image.

3.3.2 Cyclic Voltammetry (CV) of NGr-NR-SDS Composite

CV experiment is the study to obtain the current response of any material through the oxidation or reduction or both oxidation and reduction reaction [23, 24]. To investigate the current response of different composites, CV experiment was performed in 0.5 M KOH applying -0.2 to 1.4 V of potential window at 0.1 Vs-1 scan rate. Figure 5, curve a reveals the oxidation of NR, where a negligible peak observed. As NR is an insulator so it cannot contribute for the electron transfer process during the electrochemical reaction, so a small peak current is appeared at around 0.6 µA. While curve (b) represents oxidation peak of NGr-NR at around where the peak height is 11.5 µA fold larger compared to curve a. The higher current response of NGr-NR could be assigned to the outstanding electroconductivity of NGr and expanded surface area which ultimately enhance the overall conductivity of NGr-NR composite. Curve c represents the oxidation curve of NGr-NR-SDS with maximum current of around 17 µA which is the highest current compared to other composites. The highest current of NGr-NR-SDS could be attributed to the excellent electrical conductivity along with the presence of SDS which promotes the homogeneous dispersion of NGr within the NR polymeric matrix and strong attachment of NGr-NR. In addition, the presence of SDS could minimize the surface tension of NGr-

NR polymeric matrix and accelerate the ions transfer across the NGr-NR surface which ultimately enhances the electrical conductivity. Therefore, from the CV results, it can be demonstrated that the NGr-NR-SDS composite possesses the highest electrochemical response compared to other composites. The electrical response comparison between the current work and earlier publications is summed up in Table 2. The findings verify that, in comparison to earlier studies, the current investigation exhibits a larger electrical response.

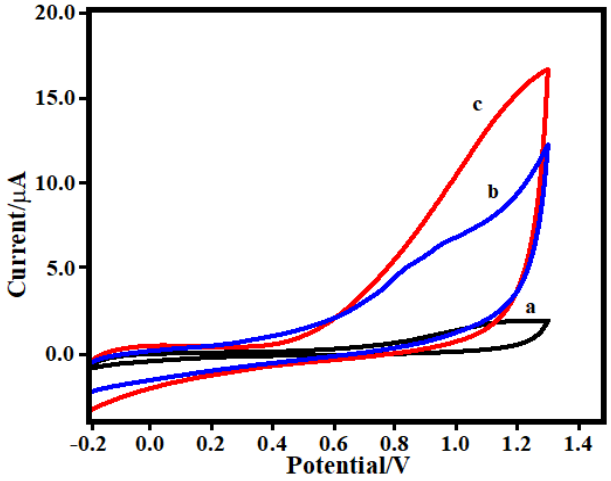

Figure 5. (A) CV responses of NR (a), NGr-NR (b) and NGr-NR-SDS (c) in 0.5 M KOH at 0.1Vs^{-1} scan rate.

3.3.3. Cyclic Stability of NGr-NR-SDS

CV experiment was conducted to study the cyclic stability of NGr-NR-SDS composite within the potential range between -0.2 to 1.4 V in the presence of 0.5 M KOH at scan rate 0.1 Vs^{-1}. Figure 6 shows that, after 15 cycles of CV, the current is almost similar and not deviated which indicates that, the NGr-NR-SDS composite possesses excellent cyclic stability.

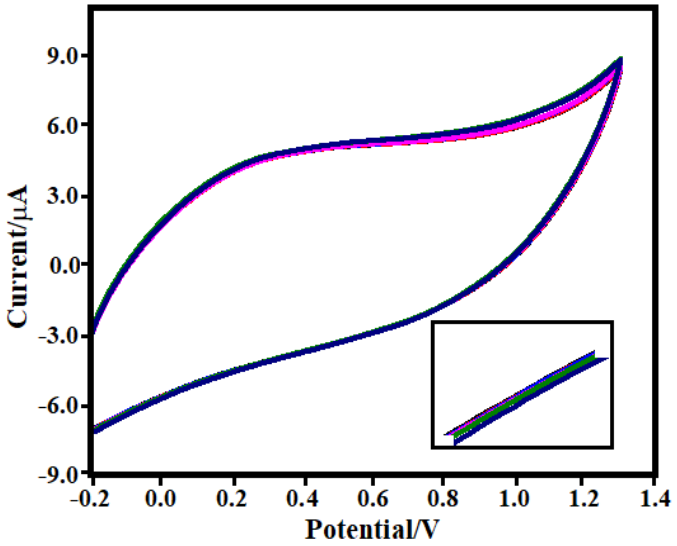

Figure 6. Cyclic stability of NGr-NR-SDS composite using 0.5 M KOH at 0.1Vs^{-1} scan rate (inset zoom in for all cycle).

Table 2 Comparative study of NGr-NR-SDS composite with previous study for electrochemical response

Composite	Effect on the Surface Morphology	Current (μA)	R_{ct} values (Ω)	Stability	Reference
CNG	Brittleness of surface	3 μA	-	-	[25]
NR-GO	Surface agglomeration	5 μA	-	-	[26]
NGr-NR-SDS	No surface Agglomeration	17 μA	1955 Ω	Excellent cyclic stability	Present work

Note: CNG: nanocellulose-graphene oxide, NR-GO: natural rubber-graphene oxide.

4. CONCLUSION

We have reported a simple, facile, and cost-efficient composite of NGr-NR-SDS using the solution blending and ultrasonication. The integration of the NGr with extra-ordinary electrical conductivity and incorporation of NR could reveal excellent cyclic stability. The presence of ionic surfactant SDS facilitates the attachment of NGr-NR and influence the electron transfer within NGr-NR by reducing the surface tension. The optimized concentration of NGr-NR-SDS composite revealed homogeneous surface morphology and composition which have been investigated through FESEM TEM, EDX and FTIR spectroscopy. The CV and EIS analysis of NGr-NR composite showed highest current response of 17 μA and lowest R_{ct} value of 1920 Ω than other composites demonstrating that the developed NGr-NR-SDS composite possesses excellent electrical conductivity, high cyclic stability and low charge transfer resistance which proves the suitability of NGr-NR-SDS as potential candidate piezoelectric composite. Therefore, the developed piezocomposite could show great flexibility and potential for the application of soft robotics, and health monitoring for different sensing applications like pressure sensors.

ACKNOWLEDGEMENTS

The authors would like to thank the Ministry of Higher Education (MoHE) Malaysia for funding this work via research grant number PRGS/1/2022/STG05/UM/02/3 (PR003-2022) and the Universiti Malaya for the funding of this research via grant number IMG006-2023. The authors also would like to thank Mrs. Hani Afiffa Binti Mohd Hanif from the Malaysia Rubber Board for supplying the natural rubber resources and Prof. Dr. Wan Jefrey Basirun from the Department of Chemistry, Faculty of Sciences, Universiti Malaya for providing the electrochemical testing facilities to support this work.

REFERENCES

[1] Akhter, S., et al., Hybrid nanocomposite of functionalized multiwall carbon nanotube, nitrogen doped graphene and chitosan with electrodeposited copper for the detection of anticancer drug nilutamide in tablet and biological samples. Materials Chemistry and Physics, 2020. **253**: p. 123393.

[2] Li, Y., et al., Ultrasensitive pressure sensor sponge using liquid metal modulated nitrogen-doped graphene nanosheets. Nano Letters, 2022. **22**(7): p. 2817-2825.

[3] Chen, A., et al., MXene@ nitrogen-doped carbon films for supercapacitor and piezoresistive sensing applications. Composites Part A: Applied Science and Manufacturing, 2022. **163**: p. 107174.

[4] Promsawat, M., et al. Effects of Poling on Electrical Properties of Flexible Piezoelectric Composites with Natural Rubber Matrix. in IOP Conference Series: Materials Science and Engineering. Vol. 553. No. 1. IOP Publishing, 2019.

[5] Marlinda, A. and M. Johan, Graphene-Polymer based Nanocomposites for Electrochemical Sensing of Toxic Chemicals. Graphene-Based Electrochemical Sensors for Toxic Chemicals, 2020. **82**: p. 186-210.

[6] Sedighi, A. and M. Montazer, Nanomaterials for Wearable, Flexible, and Stretchable Strain/Pressure Sensors. Nanotechnology in Electronics: Materials, Properties, Devices, 2023: p. 155-206.

[7] Begletsova, N., et al., The study of the stability of colloid dispersions of copper nanoparticles based on sodium dodecyl sulfate. Moscow University Chemistry Bulletin, 2019. **74**: p. 79-87.

[8] Tigari, G. and J. Manjunatha, A surfactant enhanced novel pencil graphite and carbon nanotube composite paste material as an effective electrochemical sensor for determination of riboflavin. Journal of Science: Advanced Materials and Devices, 2020. **5**(1): p. 56-64.

[9] Huang, J., et al., Extremely elastic and conductive N-doped graphene sponge for monitoring human motions. Nanoscale, 2019. **11**(3): p. 1159-1168.

[10] Liu, M.-Y., et al., Advance on flexible pressure sensors based on metal and carbonaceous nanomaterial. Nano Energy, 2021. **87**: p. 106181.

[11] Shalauddin, M., et al., Carboxylated nanocellulose dispersed nitrogen doped graphene nanosheets and sodium dodecyl sulfate modified electrochemical sensor for the simultaneous determination of paracetamol and naproxen sodium. Measurement, 2022. **194**: p. 110961.

[12] Pang, Y., et al., Preparation of lignin/sodium dodecyl sulfate composite nanoparticles and their application in pickering emulsion template-based microencapsulation. Journal of agricultural and food chemistry, 2017. **65**(50): p. 11011-11019.

[13] Zhang, J. and L. Gao, Dispersion of multiwall carbon nanotubes by sodium dodecyl sulfate for preparation of modified electrodes toward detecting hydrogen peroxide. Materials letters, 2007. **61**(17): p. 3571-3574.

[14] Li, D., et al., Facile synthesis of nitrogen-doped graphene via low-temperature pyrolysis: the effects of precursors and annealing ambience on metal-free catalytic oxidation. Carbon, 2017. **115**: p. 649-658.

[15] Shahamatifard, F., et al., Surface modification of MWCNT to improve the mechanical and thermal properties of natural rubber nanocomposites. The Canadian Journal of Chemical Engineering, 2023. **101**(4): p. 1881-1896.

[16] Radabutra, S., et al., Preparation and characterization of wood-to-wood bonding adhesive by glycidyl methacrylate grafting natural rubber. International Journal of Adhesion and Adhesives, 2022. **114**: p. 103093.

[17] Ajravat, K., S. Rajput, and L.K. Brar, Microwave assisted hydrothermal synthesis of N doped graphene for supercapacitor applications. Diamond and Related Materials, 2022. **129**: p. 109373.

[18] Lama, S., et al., Nano-sheet-like morphology of nitrogen-doped graphene-oxide-grafted manganese oxide and polypyrrole composite for chemical warfare agent simulant detection. Nanomaterials, 2022. **12**(17): p. 2965.

[19] Jiang, S., et al., Structure and properties of chitosan/sodium dodecyl sulfate composite films. RSC advances, 2022. **12**(7): p. 3969-3978.

[20] Shahmirzaee, M., et al., ZIF-8/carbon fiber for continuous adsorption of sodium dodecyl sulfate (SDS) from aqueous solutions: Kinetics and equilibrium studies. Journal of Water Process Engineering, 2021. **44**: p. 102437.

[21] Shalauddin, M., et al., Bimetallic metal organic framework anchored multi-layer black phosphorous nanosheets with enhanced electrochemical activity for paracetamol detection. Electrochimica Acta, 2023. **454**: p. 142423.

[22] Akhter, S., et al., A highly selective bifunctional nanosensor based on nanocellulose and 3D polypyrrole decorated with silver-gold bimetallic alloy to simultaneously detect methotrexate and ciprofloxacin. Sensors and Actuators B: Chemical, 2022. **373**: p. 132743.

[23] Shalauddin, M., et al., A metal free nanosensor based on nanocellulose-polypyrrole matrix and single-walled carbon nanotube: Experimental study and electroanalytical application for determination of paracetamol and ciprofloxacin. Environmental Nanotechnology, Monitoring & Management, 2022. **18**: p. 100691.

[24] Akhter, S., et al., Tri-metallic Co-Ni-Cu based metal organic framework nanostructures for the detection of an anticancer drug nilutamide. Sensors and Actuators A: Physical, 2021. **325**: p. 112711.

[25] Beeran, Yasir, et al. "Mechanically strong, flexible and thermally stable graphene oxide/nanocellulosic films with enhanced dielectric properties." *Rsc Advances* 6.54 (2016): 49138-49149.

[26] Nurhafizah, M. D., et al. "Low-temperature exfoliated graphene oxide incorporated with different types of natural rubber latex: Electrical and morphological properties and its capacitance performance." *Ceramics International* 46.5 (2020): 5610-5622.